THERMODYNAMICS OF PARTLY OCCULTED LIMB FLARES

Barbara Sylwester[1] **and Janusz Sylwester**[2]

[1]Space Research Centre, Solar Physics Division, Kopernika 11, 51-622 Wroclaw, Poland

ABSTRACT

We have studied time variations of the thermodynamic parameters for several flares which have been partly occulted by solar disc. The data consist mainly of deconvolved *Yohkoh* Soft X-ray Telescope (SXT) images coaligned to sub-arcsec accuracy using specially designed method. This method (**l**imb **p**osition **a**djustment, LPA) is based on the concept of using the edge of occulting disc as a reference in a sequence of SXT images. Spatial resolution achieved on the deconvolved images allows to derive the maps of temperature and emission measure within unocculated portion of the flaring structures (kernels) with the resolution below 1 arcsec. It is possible to estimate the electron density of plasma confined within individual kernels based on their spatial dimensions. Our analysis indicates that the hottest regions within the flaring kernels are these with the smaller density. As a rule the cooler regions are related with the denser plasma. It is typical that some amount of plasma with temperatures $T \geq 20$ MK is present within the flaring region during the rise phase. In our analysis we have followed also the maximum brightness location for pronounced flare kernels emission seen on deconvolved images. The analysis of the data reveals systematic variations of the brightest kernel position seen in the coronal portion of the active region. Derived patterns of maximum brightness location as observed on Al01, Al12 and Be119 filter images have been cross-compared with the location of hard X-ray emission centers as seen on the MEM-reconstructed Hard X-ray Telescope images. We illustrate our analysis for selected flare on 24 March 1993.

Key words: X-ray flares; thermodynamic parameters.

1. INTRODUCTION

In our present research we have used the deconvolved SXT flare images. The deconvolution is performed using Wroclaw maximum likelihood ANDRIL algorithm. The algorithm removes numerically the image blurring due to the instrument point spread function and increases the spatial resolution down to 1 arcsec. The determination of physical conditions within flaring region is a delicate matter as the analysis is **very** sensitive to the accurate coalignement between

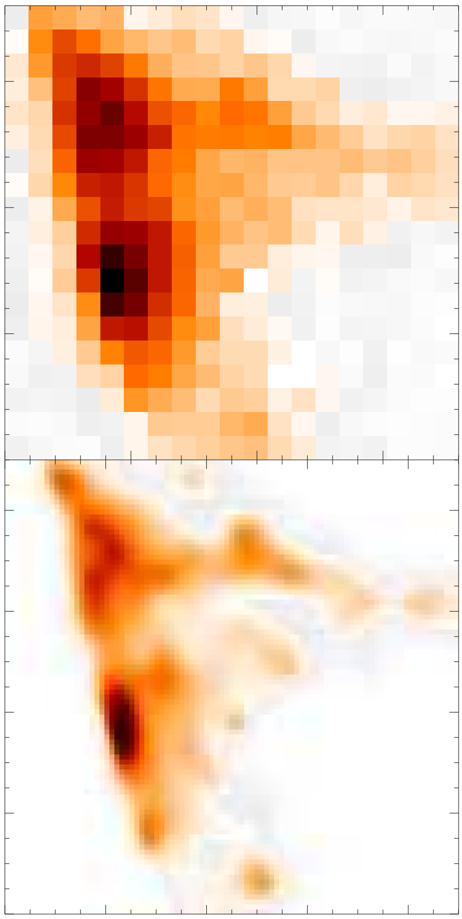

Figure 1. The comparison of the emission pattern as seen on the first available unsaturated original and deconvolved Be11 image. Only part of the image is displayed . The size of original image is 18×18 SXT pixels which correspods to 90×90 subpixels after the deconvolution.

the image pair used. As we have used the deconvolved Al12 and Be119 SXT images, the coalignement problem is of basic importance. The standard procedures of image coalignement from *Yohkoh* spacecraft attitude sensors are not accurate enough in this respect. Therefore we have applied a special method of fine image coalignement (so-called limb position adjustment, LPA) where we use the solar limb as the reference in a sequence of flare images Sylwester & Sylwester (2001). The coalignement precision with this method is of the order of 0.1 arcsec which allowed us to make the maps of distribution of physical plasma parameters for unobscured fine flaring structures (kernels) with high credibility (higher than was possible before using the procedures included in SXT_PREP package).

The deconvolved Al12 and Be119 images coaligned using LPA have been used to determine the temperature (T) and emission measure (EM) maps of the flaring unocculted region. The isothermal approximation has been adopted and filter ratio technique has been used in deriving the parameters in individual subpixels. Also the distributions of so-called "quasi" differential emission measure (QDEM) for the sequence of images have been constructed based on these results. The QDEM histogram has been obtained as follows:

- first the elements (subpixels) have been identified where the temperature falls into given (T, T+1MK) interval from the range between 5 and 30 MK,
- next the emission measures for those elements have been added and plot on the histogram.

We have also incorporate into the analysis the MEM reconstructed hard X-ray images as recorded by HXT on *Yohkoh* for the sake of comparison between soft and hard X-ray flare emission patterns. The relative soft and hard X-ray maximum brightness locations and their displacements have been investigated quantitatively.

2. DATA ANALYSIS AND RESULTS

We have analysed several limb occulted flares. As an illustration the results for selected flare which has been observed on 24 March 1993 at 03:25 UT at the Western limb are presented. This flare was of moderate duration (about 40 min.) but the *Yohkoh* observations cover 10 min. only. Although the event has not been very intense in *GOES* scale (classified as C6.6) the fluxes observed using HXT M1 channel were much above the noise level with many spikes present. In Fig. 1 one can compare the emission pattern as seen on the original and deconvolved Be11 image. The privilege of using deconvolved images is clearly seen as many fine structures not resolved on the original image are evident after the deconvolution. In Fig. 2 the composite of soft and hard

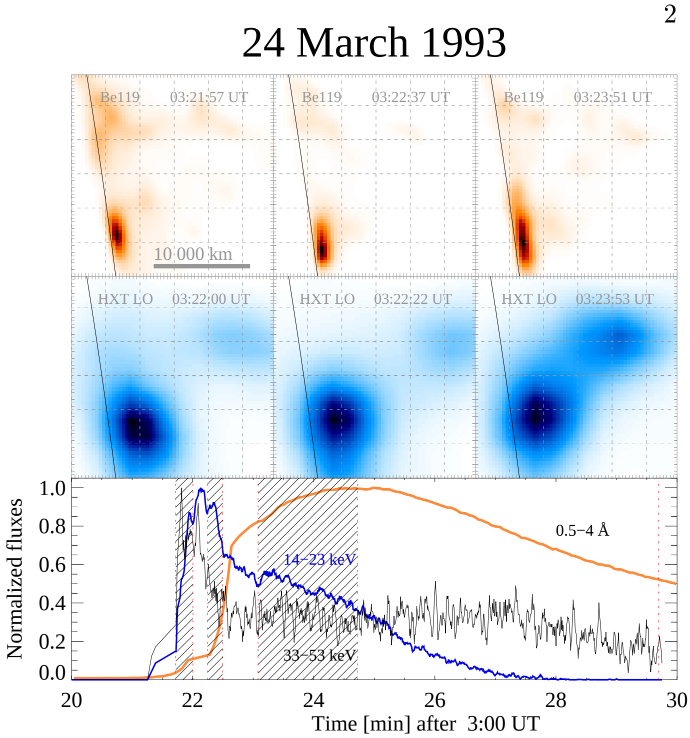

Figure 2. The composite of Be119 SXT deconvolved images (row top) and corresponding in time MEM reconstructed LO HXT images (middle row) for three moments during the rise of 24 March 1993. The soft (GOES) and hard X-ray (LO and M1 HXT) light curves are displayed at the bottom row. The hatched areas denote time intervals when the HXT fluxes have been integrated in order to reconstruct the images displayed in the middle row.

X-ray emissivity pattern for three times during the rise phase together with the soft and hard X-ray lightcurves are displayed. On the deconvolved SXT images the flare resembles a static loop-like structure with one foot/leg dominating throughout the *Yohkoh* observing period (rise, maximum and early decay phase).This event is somewhat unusual as the location of the kernel changed only slightly during its evolution. In Fig. 2 the evolution of maximum brightness location presented as contours drawn at 0.8 of maximum intensity for consecutive frames of Be119 deconvolved images is shown. The contours are overlaid atop the emission pattern (in gray) of the first unsaturated SXT image within the flaring sequence. Only a small displacement of maximum brightness location (fotpoint kernel) is observed during 10 minutes of flare evolution. Usually the location of flare kernels evidently changes as the flare evolves Sylwester & Sylwester (1999a), Sylwester & Sylwester (1999b),Sylwester & Sylwester (2001).

In Fig. 4 the distributions of main thermodynamic parameters for three moments (respective columns) during flare rise phase for the total region (upper panel) and the extracted intense foot area (lower panel) are presented. The filter ratio temperature and emission measure are presented in grey scale in the first and second rows respectively. The thin white line delimits the common statistically signifi-

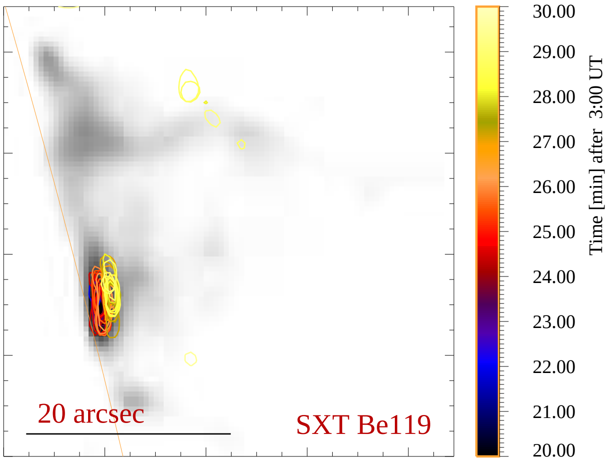

Figure 3. *The evolution of maximum brightness location (contours drawn at 0.8 of maximum intensity) for consecutive frames of Be119 deconvolved images. The contours are overlaid atop the emission pattern (in gray) of the first unsaturated Be119 image.*

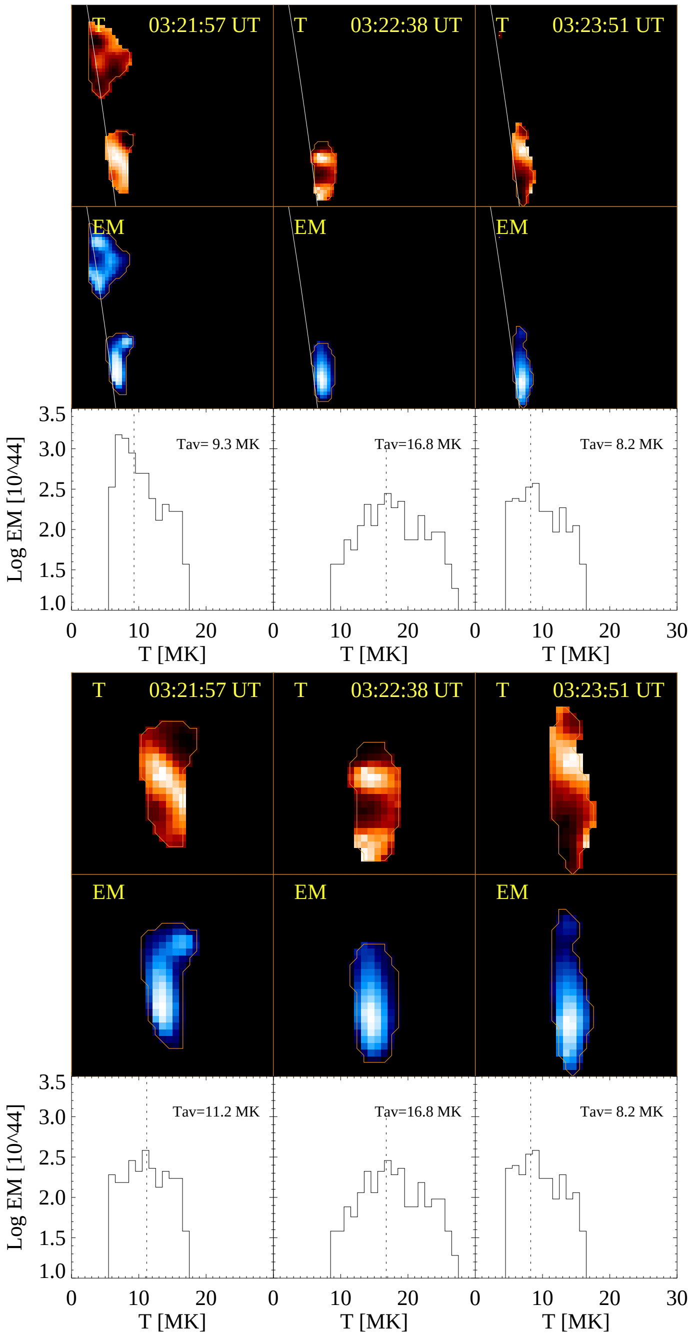

Figure 4. *The distribution of main thermodynamic parameters for three moments (respective columns) during the rise phase of GOES light curve for the total region (left panel) and the intense foot area extracted (right panel).*

cant region for Al12 and Be119 images where there is above 30 DN/subpixel (750 DN/pixel). The dimension of individual image is (30x30) arcsec and (15x15) arcsec for upper and lower panel respectively. The bottom rows in each panel show corresponding "quasi" differential emission measure distributions. The vertical dashed lines indicate the average temperature given also above the plots. It is seen that the bulk of plasma has the "typical" temperatures around 10 MK. It should be noted that using Al12 and Be119 filters the plasma with temperatures higher than 5 MK can be probed only! What is interesting is the existence of significant amount of plasma with temperatures above 20 MK during the soft X-ray rise phase, just after the main hard X-ray emission evenesced. This plasma may correspond to the so-called superhot plasma component identified from spectroscopic measurements. High-temperature tails in the QDEM distributions are no longer observed after the hard X-ray emission substantially decreases (around soft X-ray flare maximum and during soft X-ray decay phase). From spatial dimensions and the total EM it is possible to estimate the corresponding averaged densities in volumes constituting the most of soft X-ray flux. They are: 7.7×10^{10}, 2.2×10^{11} and 3.9×10^{11} cm^{-3} for total region (upper panel). The corresponding average densities for the intense foot point kernel are 1.0×10^{11}, 2.2×10^{11} and 4.0×10^{11} cm^{-3} respectively. Evidently the densities obtained are above 10^{11} cm^{-3} during most of flare evolution. (Only for the few initial frames available during the rise phase the density is below 10^{11} cm^{-3}.)

We have also compared the relative locations of the soft and hard X-ray plasma sources. It is illustrated in Fig. 5 where the comparison of SXT and HXT emission patterns (based on deconvolved and MEM reconstructed images respectively) for two moments during the flare rise phase is shown. HXT contours are overlayed atop corresponding SXT Al12 deconvolved images. The solid line correspond to LO channel emission while the dashed line relates to M1 channel emission. It is evident that the emission centers in soft and hard X-ray spectral bands are not cospatial. This was noted before for many other flares observed by *Yohkoh*.

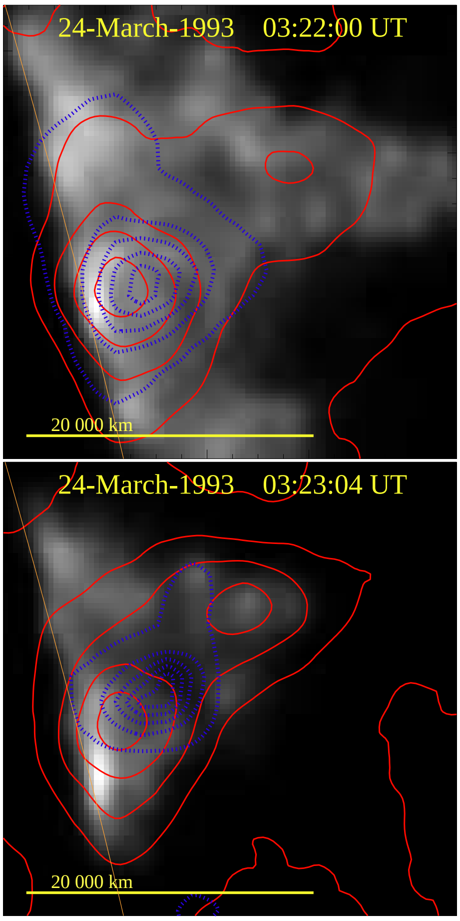

Figure 5. A sample table illustrating usage of the LATEX table environment.

3. SUMMARY

Based on the analysis of deconvolved SXT and MEM reconstructed HXT images for several limb occulted flares, the following conclusions have been drawn:

- It is possible to tune the SXT image coalignement down to fractions of arcsec using the limb position as a reference. Such a high accuracy of coalignement allows for realistic determination of the temperature structure of flaring kernels.
- Fast variations of quasi differential emission measure distribution for flaring plasma are evident. Substantial high-temperature tails ($T \geq$ 20 MK) are present during the initial flare-rise phase. These tails disappear after the flare reaches its maximum phase.
- Except of the very beginning of the flare evolution, the average density of soft X-ray sources is above 10^{11} cm^{-3}. Bright kernels are the densest volumes within flaring structures but they are also the coolest ones.
- The displacements of soft X-ray flare kernels are observed usually in the direction outward the Sun. For more intense X-ray flares the observed displacements are larger.
- As the HXT image resolution is not as good as on the deconvolved SXT images, the shape of hard X-ray source is seen as more regular and not changing during the flare evolution. However, the location of maximum hard X-ray emission changes in time which suggests a "motion" of the hot source away from the Sun.
- The location of hard X-ray emitting sources do not coincide with the positions of soft X-ray kernels even between close in energy Be119 and LO channels. The hard X-ray sources are placed sideway, usually up and above, in respect with the location of soft X-ray kernels in the most of cases.

The results presented seem hard to be accommodated for in many of the proposed theoretical scenarios for the flare phenomenon. The one which can help in understanding the results presented here is the model of flare turbulent kernel Jakimiec et al. (1998). According to this model, substantial part of energy release in the flare takes place in a bright coronal kernel with developed MHD turbulence. The energy release takes place in the relatively large volume of the kernel well into the decay phase of the flare due to magnetic reconnection within the turbulent region.

ACKNOWLEDGMENTS

This work has been supported by the Grant 2.P03D.024.17 of Polish Committee for Scientific Research.

REFERENCES

Jakimiec J., Tomczak M., Falewicz R., et al., 1998, A&A 334, 1112

Sylwester B., Sylwester J., 1999a, ESA SP-448, 895

Sylwester B., Sylwester J., 1999b, Acta Astron., 49, 85

Sylwester B., Sylwester J., 2001, Adv. Space Res., accepted